SEOULTECH
SEOUL NATIONAL UNIVERSITY OF SCIENCE & TECHNOLOGY

Computational Fluid Dynamics Lab
Department of Mechanical Engineering

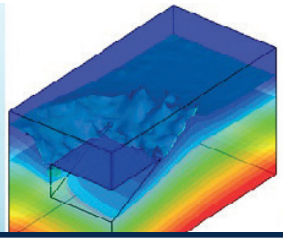

비압축성유동장의 분리기법알고리즘에 기반한 유체-구조 상호작용의 반일체(semi-monolithic) 공식화

Hyoung Gwon Choi[1*], Sang Truong Ha[2]

[1]Department of Mechanical Engineering, Seoul National University of Science and Technology.

[2]Department of Mechanical Engineering, Le Quy Don Technical University, Vietnam.

May 17th 2023

Contents

1. Preliminary to FSI
2. Governing equations
3. Partitioned, Mono, Semi-mono methods
4. Applications

FSI with application in hemodynamics

Blood flow interaction with a blood vessel in a carotid bifurcation of a rat

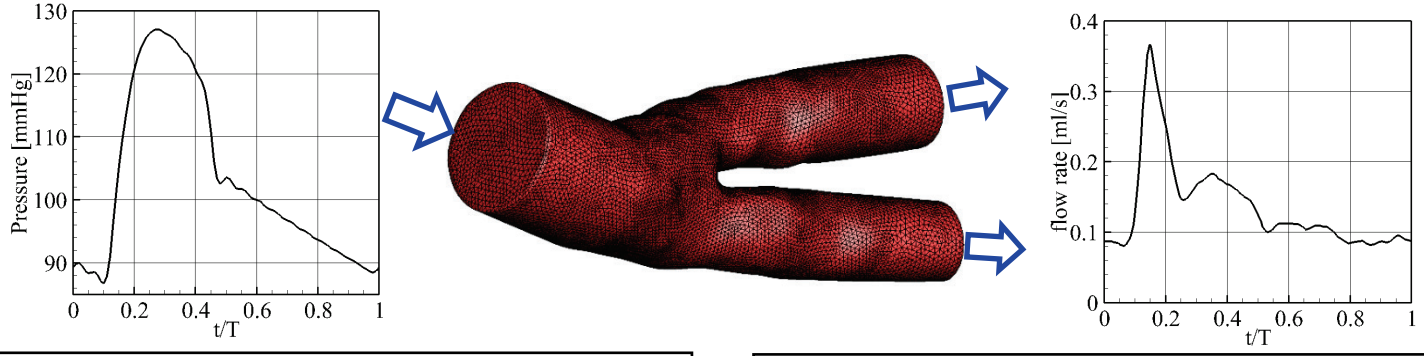

Rigid wall.

Elastic wall.

Previous studies

- 유체-구조 상호작용 해석의 중요성

장점 : 1) 혈관의 움직임을 고려함 2) 다양한 파열 예측 인자를 얻을 수 있음.

단점 : 계산량이 많기 때문에 유동만 고려하는 해석보다 약 20배 이상 느림. [1]

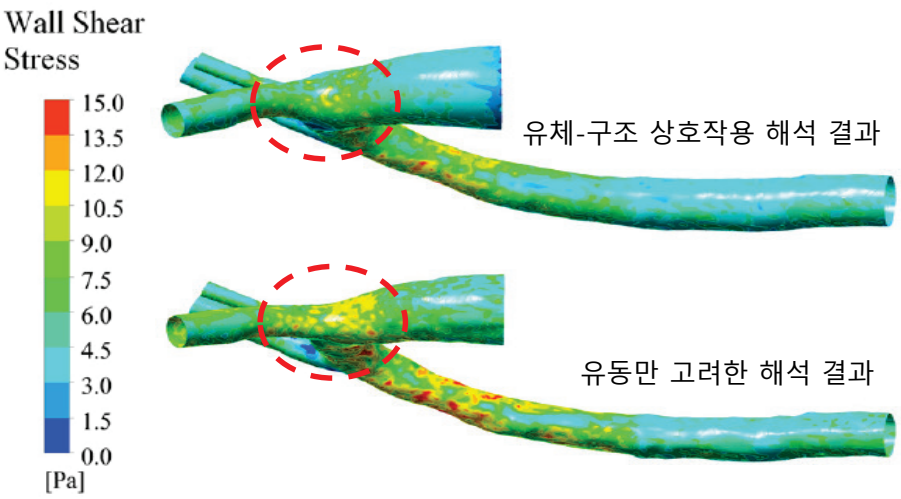

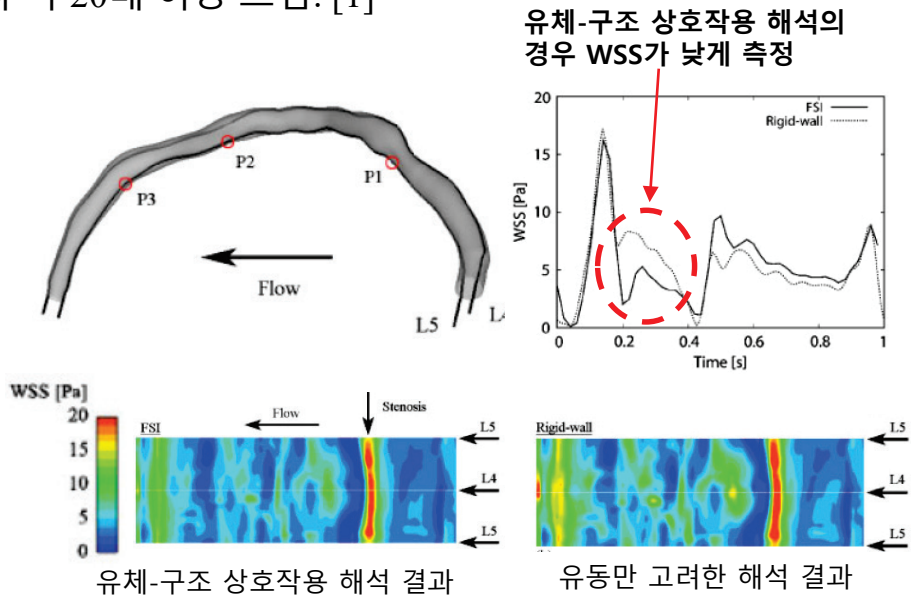

유체-구조 상호작용 해석 유무에 따른 벽전단응력 결과 비교[1],[2]

[1] A.G. Brown et al., “Accuracy vs. computational time : Translating arotic simulations to the clinic”, Journal of Biomechanics, Vol. 45, pp. 516-523, 2012.

[2] R. Torii et al., “Fluid-structure interaction analysis of a patient-specific right coronary artery with physiological Velocity and pressure waveforms”, Communications in Numerical Methods in Engineering, Vol. 25, pp. 565-580, 2009.

Mono vs. Staggered Algorithm

- Staggered algorithm

$$\begin{bmatrix} M_f & G \\ G^T & 0 \end{bmatrix} \begin{bmatrix} u_f \\ P_f \end{bmatrix} = \begin{bmatrix} \mathsf{F}_f \\ 0 \end{bmatrix}$$

✚ Interface coupling

$$[M_S][d_S] = [\mathsf{F}_S]$$

$$u_f = \frac{\partial d_S}{\partial t} \quad on \ \ \Gamma$$

- Monolithic algorithm (Combined formulation)

$$\begin{bmatrix} M_f & G & C_{fS} \\ G^T & 0 & 0 \\ C_{SV} & C_{SP} & M_S \end{bmatrix} \begin{bmatrix} u_f \\ P \\ \dot{d}_S \end{bmatrix} = \begin{bmatrix} \mathsf{F}_f \\ 0 \\ \mathsf{F}_S \end{bmatrix}$$

$$\boldsymbol{\sigma}_f \cdot \mathbf{n}_f + \boldsymbol{\sigma}_s \cdot \mathbf{n}_s = 0 \quad on \ \ \Gamma$$

Partitioned method solving Fluid-Structure Interaction problems

Partitioned (staggered) method => Iteration algorithm is used

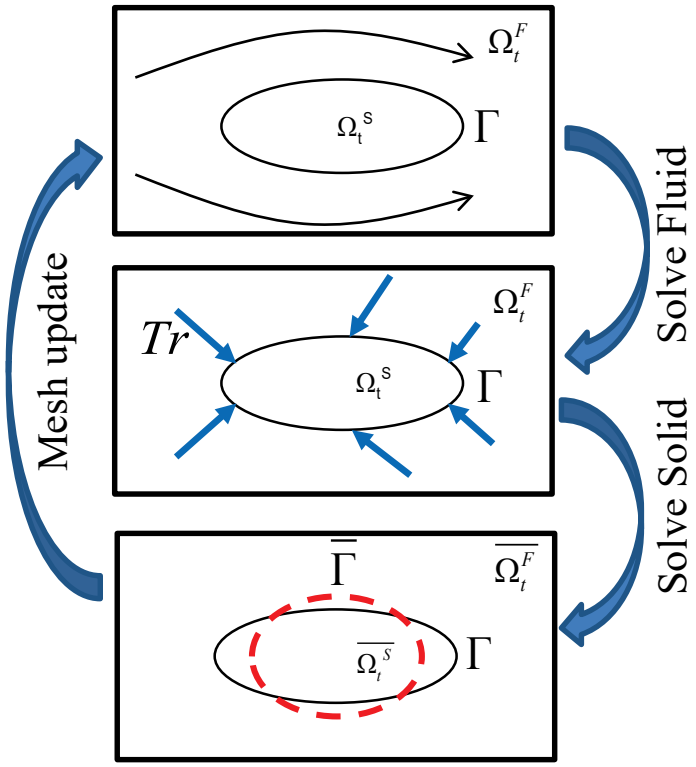

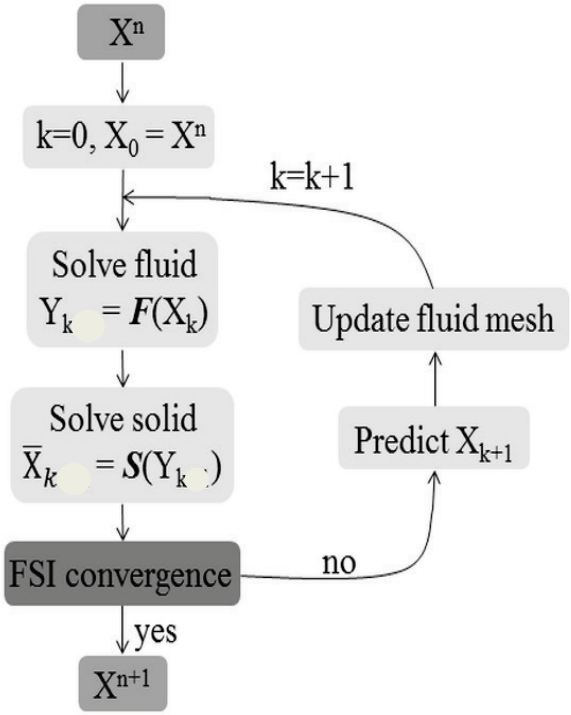

Flow chart of FSI algorithm

Denote: $\mathbf{X}_k$ *is a predicted variable on interface (displacement)* at *kth*-(FSI) iteration of time level *n*

The solution vector after solving FSI

$\bar{\mathbf{X}}_k = \mathbf{S}\circ\mathbf{F}\,(\mathbf{X}_k)$;

FSI Error $\mathbf{r_k} = \bar{\mathbf{X}}_k - \mathbf{X}_k$

If $\| \mathbf{r_k} \| < \varepsilon \Rightarrow$ ***FSI*** *convergence* $\Rightarrow$ *exit*

Otherwise predict $\mathbf{X}_{k+1}$ *for next FSI iteration*

Governing equations

- Fluid flow (ALE form):

$$\begin{cases} \nabla \cdot \mathbf{v}^f = 0, \\ \rho^f \left[\dfrac{\partial \mathbf{v}^f}{\partial t} + \left(\mathbf{v}^f - \mathbf{v}^m \right) \cdot \nabla \mathbf{v}^f \right] = -\nabla p + \nabla \cdot \boldsymbol{\tau}, \qquad \boldsymbol{\tau} = \mu \left[\nabla \mathbf{v}^f + \left(\nabla \mathbf{v}^f \right)^T \right] \end{cases} \tag{1}$$

- Elastic structure:

$$\nabla . \sigma + \rho b = \rho \frac{\partial^2 u}{\partial t^2} \tag{2}$$

σ : Cauchy stress tensor

- Constitutive equations

linear elastic structure (small deformation)

$$\begin{cases} \boldsymbol{\sigma} = \mathbf{c} : \boldsymbol{\varepsilon} \\ \boldsymbol{\varepsilon} = \dfrac{1}{2} \left[\left(\nabla \mathbf{u}^s \right) + \left(\nabla \mathbf{u}^s \right)^T \right] \end{cases} \tag{3}$$

ε: Strain tensor

Governing equations

- Nonlinear (*) (Large deformation) $S = \mathbb{C} : E = JF^{-1}\sigma F^{-T}$ $T = JF^{-1}\sigma$

S is the second Piola-Kirchhoff stress tensor

Right Cauchy deformation tensor C: $C=F^{T}F$ Deformation tensor $F = I+\nabla_X \mathbf{u}$ $J = \det(F)$

Non-linear term

Green strain tensor E: $E = \frac{1}{2}(C-I) = \frac{1}{2}[(\nabla_X \mathbf{u})^{T} + (\nabla_X \mathbf{u}) + (\nabla_X \mathbf{u})^{T} \cdot (\nabla_X \mathbf{u})]$

❖ Total Lagrangian formulation $\nabla_X . T + \rho_0 b = \rho_0 \frac{\partial^2 u}{\partial t^2}$

All variables corresponding to the initial configuration (t=0)

❖ Updated Lagrangian formulation $\nabla . S + \rho b = \rho \frac{\partial^2 u}{\partial t^2}$

All variables corresponding to the current configuration (t)

(*) Peter Wriggers, Nonlinear Finite Element Methods

Governing equations

Hyper-elastic material

$S = \mathbb{C} : E$ $\mathbb{C}$: Non-linear material tensor

Stress and material tensors can be calculated from elastic strain energy (ψ):

$$S = \frac{\partial \psi}{\partial E}; \quad \mathbb{C} = \frac{\partial S}{\partial E} = \frac{\partial^2 \psi}{\partial E \partial E}$$

Or $$S = 2\frac{\partial \psi}{\partial C}; \quad \mathbb{C} = 2\frac{\partial S}{\partial C} = 4\frac{\partial^2 \psi}{\partial C \partial C}$$

Mooney-Rivlin model

Linear MR: $$\psi = \frac{\mu_1}{2}(\bar{I}_1 - 3) + \frac{\mu_2}{2}(\bar{I}_2 - 3) + \frac{k}{2}(J-1)^2$$

High-order(*)

$$\begin{aligned}\psi = {} & c_{10}(\bar{I}_1 - 3) + c_{01}(\bar{I}_2 - 3) + c_{20}(\bar{I}_1 - 3)^2 + c_{11}(\bar{I}_1 - 3)(\bar{I}_2 - 3) \\ & + c_{02}(\bar{I}_2 - 3)^2 + c_{30}(\bar{I}_1 - 3)^3 + c_{21}(\bar{I}_1 - 3)^2(\bar{I}_2 - 3) \\ & + c_{12}(\bar{I}_1 - 3)(\bar{I}_2 - 3)^2 + c_{03}(\bar{I}_2 - 3)^3 + \frac{k}{2}(J-1)^2\end{aligned}$$

where $\bar{I}_1, \bar{I}_2$, Jare the invariants of C

(*) S.T. Ha and H.G. Choi, Investigation on the effect of density ratio on the convergence behavior of partitioned method for fluid–structure interaction simulation, JFS 2020.

Main publication lists of FSI algorithm

1. **Monolithic method (2012, *International journal for numerical methods in engineering*)**

   S. Kang, H. G. Choi, J. Y. Yoo, "Investigation of fluid–structure interactions using a velocity-linked P2/P1 finite element method and the generalized-α method"

2. **Partitioned method (2020, *Journal of Fluids and Structures*)**

   S. T. Ha & H. G. Choi, "Investigation on the effect of density ratio on the convergence behavior of partitioned method for fluid–structure interaction simulation"

3. **Semi-implicit method (2023, *Journal of Mechanical Science and Technology*)**

   S. T. Ha, H. G. Choi, N. C. Long, S. W. Lee, "A semi-implicit finite element formulation of the partitioned method for fluid-structure interaction based on a flux boundary condition of pressure equation"

4. **Semi-monolithic method (2023, *Computers & Mathematics with Applications*)**

   S. T. Ha & H. G. Choi, "Semi-monolithic formulation based on a projection method for simulating fluid–structure interaction problems"

Partitioned method solving Fluid-Structure Interaction problems

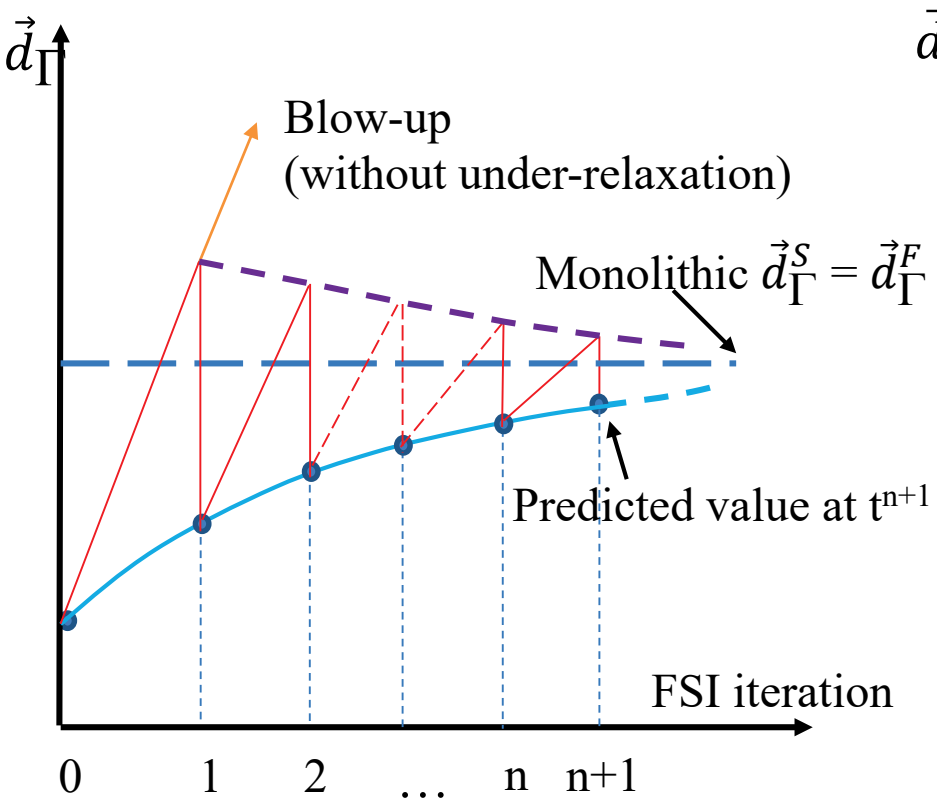

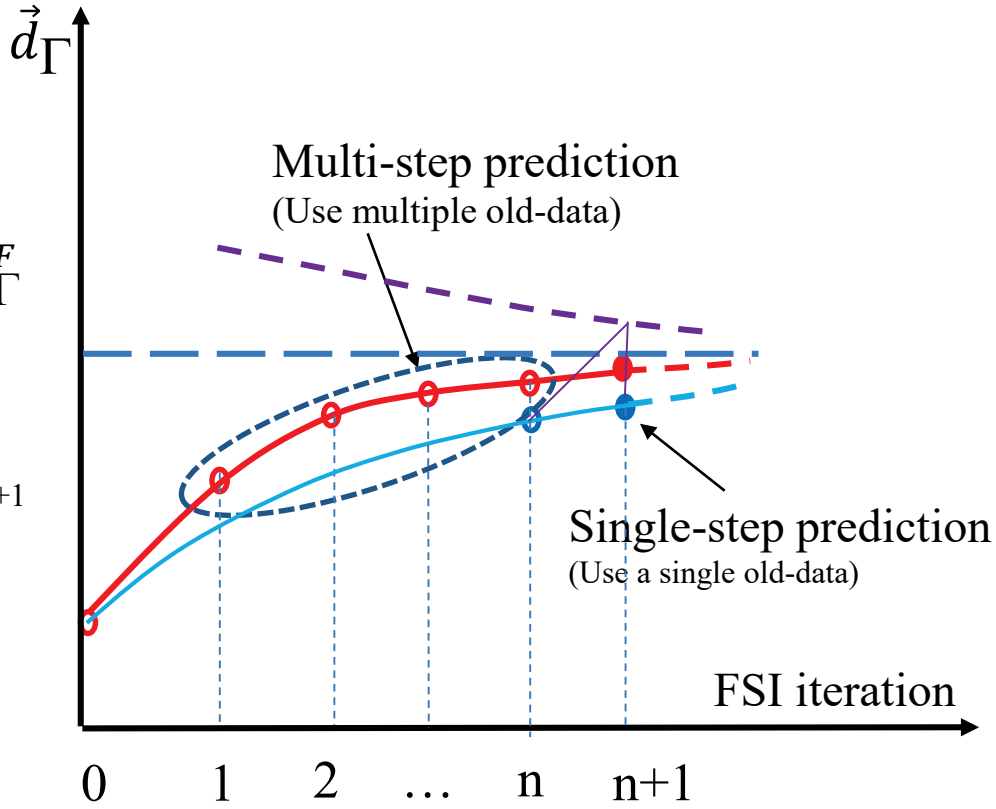

Partitioned method solving Fluid-Structure Interaction problems

The formulations

1- Fixed relaxation $\mathbf{X}^{k+1} = \omega * \bar{\mathbf{X}}^{k} + (1-\omega)*\mathbf{X}^{k}$, $0 < \omega < 1$

Or $\mathbf{X}^{k+1} = \mathbf{X}^{k} + \omega*\mathbf{r}^{k}$ Where $\mathbf{r}^{k} = \bar{\mathbf{X}}^{k} - \mathbf{X}^{k}$

Incremental vector

$\mathbf{X}^{k}$: predicted value of current iteration

$\bar{\mathbf{X}}^{k}$: Solution of current iteration: $\bar{\mathbf{X}}^{k} = \mathbf{S}\circ\mathbf{F}(\mathbf{X}^{k})$

$\mathbf{X}^{k+1}$: predicted value of next iteration

2- Aitken's relaxation (adaptive relaxation) [1] $\omega_{k+1} = -\omega_{k} \dfrac{(\mathbf{r}^{k-1})^{\mathrm{T}}(\mathbf{r}^{k} - \mathbf{r}^{k-1})}{\left|\mathbf{r}^{k} - \mathbf{r}^{k-1}\right|^{2}}$

$\mathbf{X}^{k+1} = Function\ (\bar{\mathbf{X}}^{k}, \bar{\mathbf{X}}^{k-1}, \mathbf{X}^{k}, \mathbf{X}^{k-1})$

[1] Ulrich Küttler et al, 2008, Fixed-point fluid–structure interaction solvers with dynamic relaxation.

Staggered formulation (rigid-body): Kleefsman et al ; JCP : 2005. (COMSOL)

$$\mathbf{a}_B = \frac{1}{m_B}\mathbf{F}_B$$

1. Explicit (Staggered) (Unstable)

$$\mathbf{a}_B^{n+1} = \frac{1}{m_B}\mathbf{F}_B^{n} \qquad \text{----- (1)}$$

$$\mathbf{a}_B^{n+1} = \frac{m_a}{m_B}\mathbf{a}_B^{n} \qquad \text{----- (2)}$$ (Assume $\mathbf{F}_B^{n} \sim m_a \mathbf{a}_B^{n}$ by inertial force dominant)

(2) Is stable only when $m_a \ll m_b$

2. iterative (Staggered) with under relaxation. So, [Iteration with Under relaxation] is introduced

$$\mathbf{a}_B^{n+1} = \left(\mathbf{V}_B^{n+1} - \mathbf{V}_B^{n}\right)/\delta t$$

$$\left(\mathbf{V}_B^{n+1}\right)^{k+1} = \mathbf{V}_B^{n} + \frac{\delta t}{m}\mathbf{F}_B^{k}$$, using relaxation

$$\left(\mathbf{V}_B^{n+1}\right)^{k+1} = \left(\mathbf{V}_B^{n+1}\right)^{k} + \omega\left(\left(\mathbf{V}_B^{n+1}\right)^{*} - \left(\mathbf{V}_B^{n+1}\right)^{k}\right)$$

$$\therefore \left(\mathbf{V}_B^{n+1}\right)^{k+1} = \omega\left(\mathbf{V}_B^{n} + \frac{\delta t}{m}\mathbf{F}_B^{k}\right) + (1-\omega)\left(\mathbf{V}_B^{n+1}\right)^{k}$$

k ~ up to 20 for lighter body ?

Partitioned method solving Fluid-Structure Interaction problems

3- QN_ILS [2] : Quasi-Newton with Inverse Jacobian from a Least-Squares model

$$\mathbf{X}^{k+1} = \mathbf{X}^k + \Delta\mathbf{X}^{k+1} = \mathbf{X}^k + \Delta\bar{\mathbf{X}}^{k+1} - \Delta\mathbf{r}^{k+1}$$

$$\mathbf{r} = \bar{\mathbf{X}} - \mathbf{X}, \Delta\bar{\mathbf{X}}^i = \bar{\mathbf{X}}^i - \bar{\mathbf{X}}^k$$

$$\Delta\bar{\mathbf{X}}^{k+1} \approx \sum_{i=1}^{k-1} \Delta\bar{\mathbf{X}}^i * c^i$$

$$\Delta\mathbf{r}^{k+1} = \mathbf{r}^{k+1} - \mathbf{r}^k \approx -\mathbf{r}^k$$

$$\Rightarrow \quad \mathbf{X}^{k+1} = \mathbf{X}^k + \sum_{i=1}^{k-1} \Delta\bar{\mathbf{X}}^i * c^i + \mathbf{r}^k$$

Parameters c^i

$$-\mathbf{r}^k \approx \Delta\mathbf{r}^{k+1} \approx \sum_{i=1}^{k-1} \Delta\mathbf{r}^i * c^i = [\mathbf{V}] \times \mathbf{c}$$

$$\Delta\mathbf{r}^i = \mathbf{r}^i - \mathbf{r}^k (1 \le i \le k-1)$$

Least-square method is used to minimize $\mathbf{R}(\mathbf{c}) = [\mathbf{V}] \times \mathbf{c} + \mathbf{r}^k$

$$\frac{\partial \mathbf{R}(\mathbf{c})}{\partial \mathbf{c}} = \mathbf{0}$$

$$\Rightarrow \quad \mathbf{c} = (\mathbf{V}^T\mathbf{V})^{-1}\mathbf{V}^T(-\mathbf{r}^k)$$

If only one previous value is considered:

$$\mathbf{X}^{k+1} = \mathbf{X}^k + \Delta\bar{\mathbf{X}}^{k-1} * c^{k-1} + \mathbf{r}^k = \mathbf{X}^k + (\tilde{\bar{\mathbf{X}}}^{k-1} - \bar{\mathbf{X}}^k) * c^{k-1} + \mathbf{r}^k$$

$$\approx \mathbf{X}^k + (\mathbf{X}^k - \bar{\mathbf{X}}^k) * c^{k-1} + \mathbf{r}^k = \mathbf{X}^k + \underbrace{(1 - c^{k-1})}_{\omega} * \mathbf{r}^k$$

[2] Joris Degroote et al, 2010 , Performance of partitioned procedures in fluid–structure interaction. Computers and Structures Vol.88, p.446-457.

Semi-Implicit method

✓ Semi-Implicit based on Projection scheme [4]

- Second order extrapolation of the fluid-structure interface:

$$\tilde{\mathbf{d}}^{n+1} = \mathbf{d}^n + \Delta t\left(\frac{3}{2}\dot{\mathbf{d}}^n - \frac{1}{2}\dot{\mathbf{d}}^{n-1}\right)$$

- Mesh moving:

$$\begin{cases} \nabla^2 \mathbf{w}^{n+1} = 0, & \text{in } \Omega^f \\ \mathbf{w}^{n+1} = \dfrac{\tilde{\mathbf{d}}^{n+1} - \mathbf{d}^n}{\Delta t}, & \text{on } \Sigma\ ; \end{cases}$$

- Definition of the new domain:

$$\Omega^{f,n+1} = \Omega^{f,n} + \Delta t.\, w^{n+1}$$

- Advection-diffusion step (explicit)

$$\begin{cases} \rho^f \dfrac{\tilde{\mathbf{u}}^{n+1} - \mathbf{u}^n}{\Delta t} + \rho^f (\tilde{\mathbf{u}}^n - \mathbf{w}^{n+1}) \cdot \nabla \tilde{\mathbf{u}}^{n+1} - \mu \nabla \cdot [\nabla \tilde{\mathbf{u}}^{n+1} + (\nabla \tilde{\mathbf{u}}^{n+1})^T] = 0, & \text{in } \Omega^{f,n+1} \\ \tilde{\mathbf{u}}^{n+1} = \mathbf{w}^{n+1}, & \text{on } \Sigma^{n+1} \end{cases}$$

[4] Jean-Frederic Gerbeau et al. 'A projection semi-implicit scheme for the coupling of an elastic structure with an incompressible fluid '. *IJNME (2007)*

Semi-Implicit method

✓ Semi-Implicit based on Projection scheme

- Implicit coupling:

Fluid domain

$$\begin{cases} \rho^f \dfrac{\mathbf{u}^{n+1}-\tilde{\mathbf{u}}^{n+1}}{\Delta t} + \nabla p^{n+1} = 0, & \text{in } \Omega^{f,n+1} \\ \nabla \cdot \mathbf{u}^{n+1} = 0, & \text{in } \Omega^{f,n+1} \\ \mathbf{u}^{n+1} \cdot \mathbf{n}^f = \dfrac{\mathbf{d}^{n+1}-\mathbf{d}^n}{\Delta t} \cdot \mathbf{n}^f, & \text{on } \Sigma^{n+1} \end{cases}$$

Solid domain

$$\begin{cases} \rho^s \dfrac{\dot{\mathbf{d}}^{n+1}-\dot{\mathbf{d}}^n}{\Delta t} - \square\, \boldsymbol{\sigma}_s^{n+1} = 0, & \text{in } \Omega^{s,n+1} \\ \boldsymbol{\sigma}_s^{n+1} \cdot \mathbf{n}^s = \boldsymbol{\sigma}_f^{n+1}(\tilde{\mathbf{u}}^{n+1}, p^{n+1}) \cdot \mathbf{n}^s, & \text{on } \Sigma^{n+1} \end{cases}$$

Semi-Implicit method

Semi-implicit using pressure Poisson equations

Step 4: Strong-coupling partitioned method of pressure variable and solid displacement

Sub-step 1: Pressure solver:

$$\begin{cases} \nabla^2 \mathrm{p}^{n+1} = \frac{\rho}{\Delta t} \nabla \cdot \mathbf{u}^* & \text{in } \Omega^f \\ \mathbf{u}^{n+1} = \dfrac{\mathbf{d}^{n+1} - \mathbf{d}^n}{t} & \text{on } \Gamma^{fs} \end{cases}$$

$$\Rightarrow \quad \boxed{\int_{\Omega} \nabla q \,.\, \nabla \mathrm{p}^{n+1}\, d\Omega = \frac{\rho}{\Delta t}\left\{ \int_{\Omega} \nabla q \,.\, \mathbf{u}^* d\Omega - \int_{\Gamma} q\, \mathbf{u}^{n+1} \,.\, \mathbf{n} d\Gamma \right\}}$$

Sub-step 2: Solid displacement solver:

$$\begin{cases} \rho^s \dfrac{\dot{\mathbf{d}}^{n+1} - \dot{\mathbf{d}}^n}{\Delta t} - \square\, \boldsymbol{\sigma}_s^{n+1} = 0, & \text{in } \Omega^{s,n+1} \\ \boldsymbol{\sigma}_s^{n+1} \cdot \mathbf{n}^s = \boldsymbol{\sigma}_f^{n+1}(\tilde{\mathbf{u}}^{n+1}, p^{n+1}) \cdot \mathbf{n}^s, & \text{on } \Sigma^{n+1} \end{cases}$$

Step 5: Update of fluid velocity

$$\mathbf{u}^{n+1} = \mathbf{u}^* - \frac{\Delta t}{\rho} \nabla \mathrm{p}^{n+1} \text{ in } \Omega^f$$

Semi-monolithic method (version 3 FSI)

Monolithic method for Strong-coupling Pressure and displacement

Step 4: Strong-coupling method of pressure variable and solid displacement (the other steps are unchanged).

Pressure:

$$\begin{cases} \nabla^2 \mathrm{p}^{n+1} = \frac{\rho}{\Delta t} \nabla \cdot \mathbf{u}^* & \text{in } \Omega^f \\ \mathbf{u}^{n+1} = \dfrac{\mathbf{d}^{n+1} - \mathbf{d}^n}{\Delta t} & \text{on } \Gamma^{fs} \end{cases}$$

Solid displacement:

$$\begin{cases} \rho^s \dfrac{\dot{\mathbf{d}}^{n+1} - \dot{\mathbf{d}}^n}{\Delta t} - \square\, \boldsymbol{\sigma}_s^{n+1} = 0, & \text{in } \Omega^{s,n+1} \\ \boldsymbol{\sigma}_s^{n+1} \cdot \mathbf{n}^s = \boldsymbol{\sigma}_f^{n+1}(\tilde{\mathbf{u}}^{n+1}, p^{n+1}) \cdot \mathbf{n}^s, & \text{on } \Sigma^{n+1} \end{cases}$$

FEM formula:

$$\begin{cases} \displaystyle\int_\Omega \nabla q \cdot \nabla \mathrm{p}^{n+1}\, d\Omega + \frac{\rho}{(\Delta t)^2} \int_{\Gamma^{fs}} q\, d(\mathbf{d}) \cdot \mathbf{n} d\Gamma = \frac{\rho}{\Delta t} \left\{ \int_\Omega \nabla q \cdot \mathbf{u}^* d\Omega - \int_{\Gamma_D^v} q\, \tilde{\mathbf{u}} \cdot \mathbf{n} d\Gamma \right\} - \frac{\rho}{(\Delta t)^2} \int_{\Gamma^{fs}} q\, (\mathbf{d}^{n+1,i} - \mathbf{d}^n) \cdot \mathbf{n} d\Gamma \\ [\bar{\mathbf{G}}^s] d(\mathbf{d})^{n+1,i+1} + \boldsymbol{\sigma}_f^{n+1}(\tilde{\boldsymbol{u}}^{n+1}, p^{n+1}) \cdot \boldsymbol{n}^f = (\mathbf{P}^s)^n - (\mathbf{Q}^s)^{n+1,i} \end{cases}$$

$(\Delta \mathbf{d} = d(\mathbf{d}) = \boldsymbol{d}^{n+1,i+1} - \boldsymbol{d}^{n+1,i})$

$$\Rightarrow \boxed{\begin{aligned} \tilde{L}\mathrm{p} + \tilde{\Gamma} \Delta \mathbf{d}^{fs} &= \mathbf{F}_\mathrm{p} \\ \tilde{T}_r \mathrm{p}^{fs} + \tilde{G} \Delta \mathbf{d} &= \mathbf{F}_\mathrm{d} \end{aligned}} \Rightarrow \begin{bmatrix} \tilde{L} & \tilde{\Gamma} \\ \tilde{T}_r & \tilde{G} \end{bmatrix} \begin{bmatrix} \mathrm{p} \\ \Delta \mathbf{d} \end{bmatrix} = \begin{bmatrix} \mathbf{F}_\mathrm{p} \\ \mathbf{F}_\mathrm{d} \end{bmatrix}$$

Application for simulating blood vessel

2D flow in a circular channel (T_c = 0.2 s, dt = 2x10^{-3} s)

$$T_c = \frac{L_c}{\sqrt{\frac{E}{\rho}}}$$

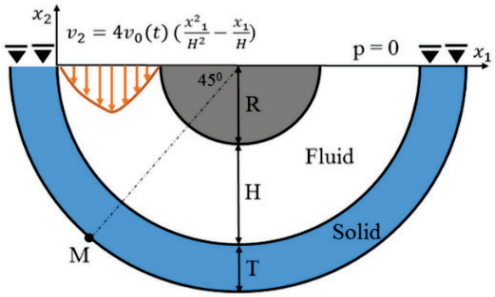

Schematic of the flow in a circular channel

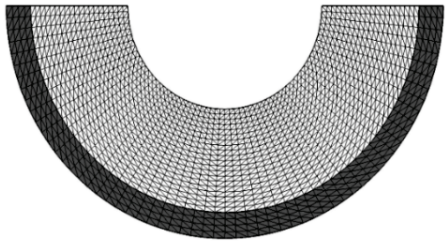

Grids of fluid and solid

CPU time normalised by that of the semi-implicit method

FSI algorithms	ANSYS	Aitken's method	QN-ILS	Semi-implicit method	Monolithic method
CPU time	**(44)**	**(9.6)**	**(3.1)**	**(1)**	**(1.6)**

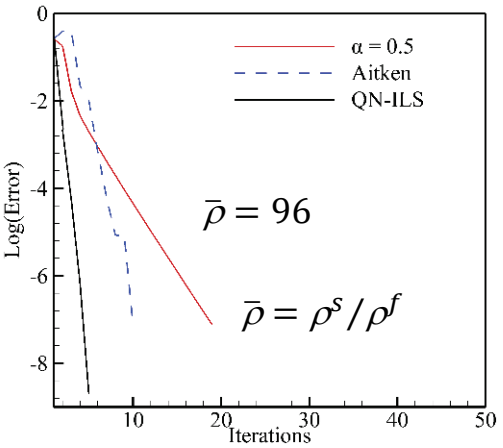

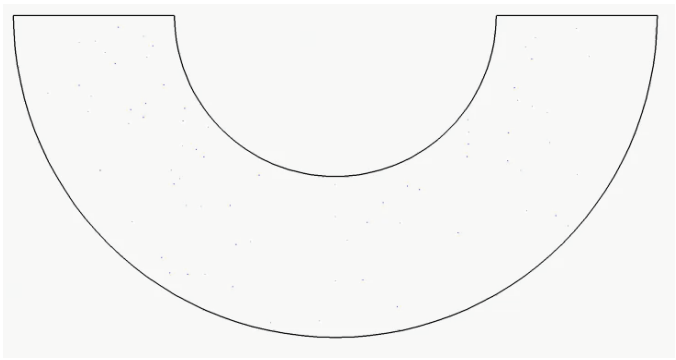

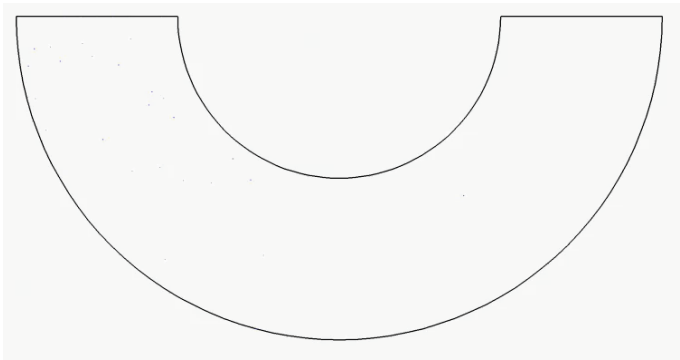

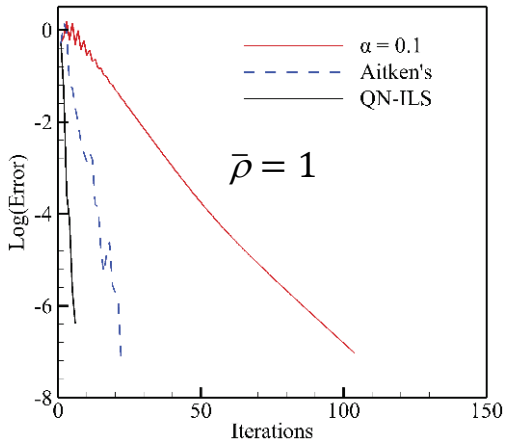

Heavy solid $\bar{\rho} = 96$

Light solid $\bar{\rho} = 1$

Convergence histories at time = 1.2 s

Application for simulating blood vessel

2D flexible beam behind a cylinder (T_c = 0.01 s, dt = 5x10^{-4} s)

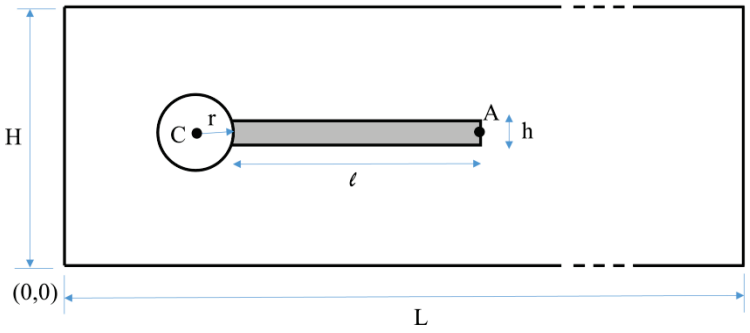

The schematic of the 2D simulation.

Dimension of the simulation domain		
Dimension		Value [m]
Channel Width	H	0.41
Channel Length	L	2.5
Cylinder Radius	r	0.05
Flag Length	l	0.35
Flag Width	h	0.02
Cylinder Center	C	(0.2,0.2)
Reference point	A	(0.6,0.2)

CPU time normalised by that of the semi-implicit method in 2D problem

FSI algorithms	Semi-implicit partitioned	Implicit partitioned	Monolithic method
CPU time	1.0	3.1	1.6

Application for simulating blood vessel

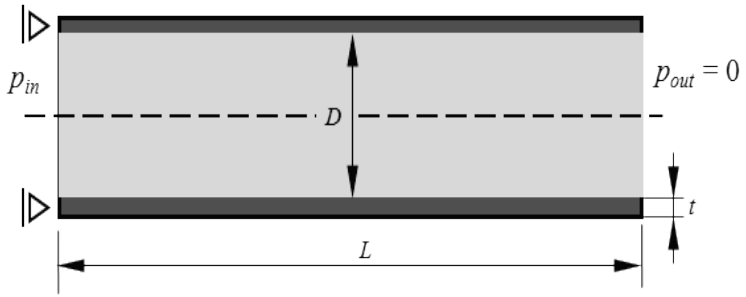

Flexible pipe configuration

$T_c = 2x10^{-2}$ s; $dt = 1x10^{-4}$ s

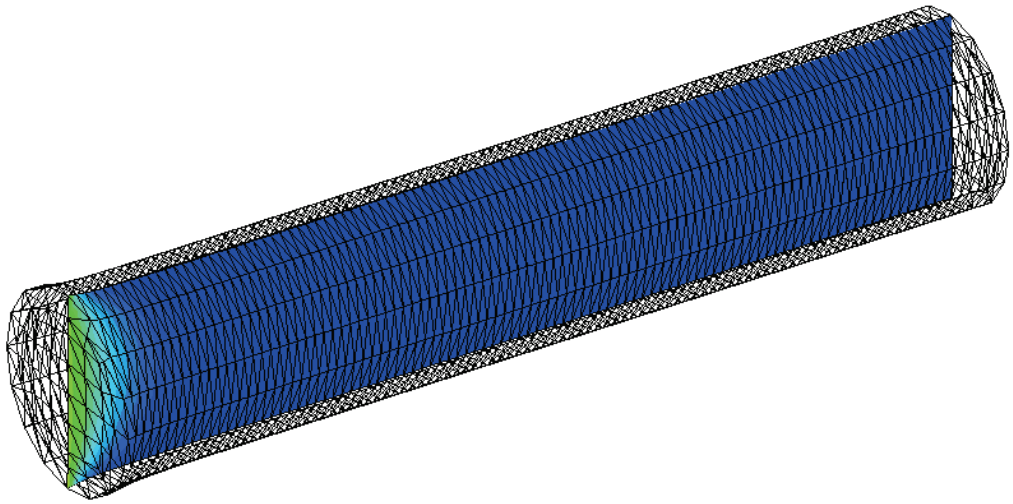

Geometry			
$L = 0.1\ m$	$D = 0.02\ m$	$t = 0.002\ m$	
Material properties			
Fluid	$\rho_f = 1000\ kg/m^3$	$\mu = 0.004\ Pa.s$	
Solid	$\rho_s = 1000\ kg/m^3$	$E = 1.0e6\ Pa$	$\nu = 0.3$

CPU time for 80 time-steps					
Solvers	ANSYS	Aitken's method	QN-ILS	Semi-implicit method	Monolithic method
CPU Time (hours)	12.28 (**52**)	3.52 (**14**)	0.85 (**3.6**)	0.24 (**1**)	0.41 (**1.7**)

Application for simulating blood vessel

Flow in 3D straight flexible tube

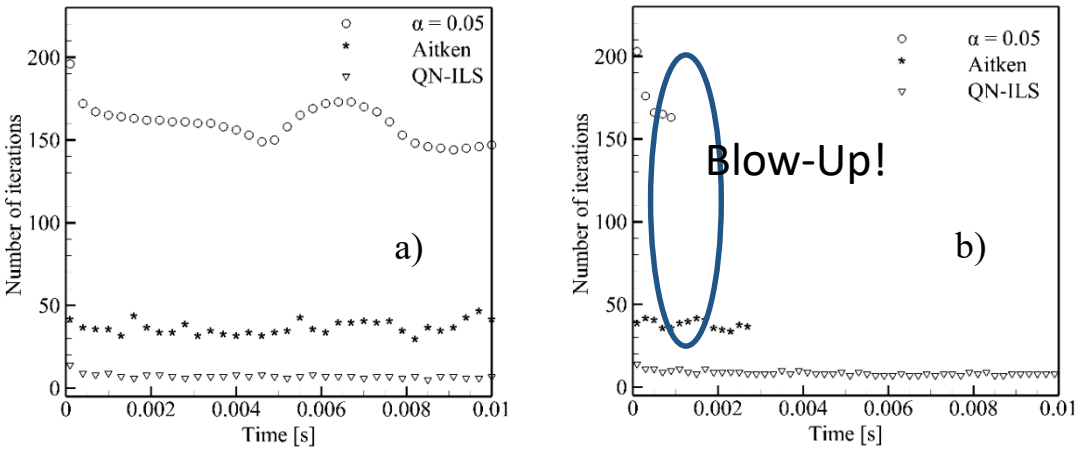

The number of FSI coupling versus time;
a) small displacement, b) large displacement

- The QN-ILS is much faster than others
- In large displacement case: fixed under-relaxation and Aitken's were divergence.

- With a heavy solid ($\bar{\rho} = 10$) there are not big different of partitioned methods in terms of convergence behaviour
- With same density case($\bar{\rho} = 1.2$): QN-ILS is much faster than others methods
- With slight solid ($\bar{\rho} = 0.5$): Fixed-relaxation very poor.
- QN_ILS is comparable with monolithic method [3]

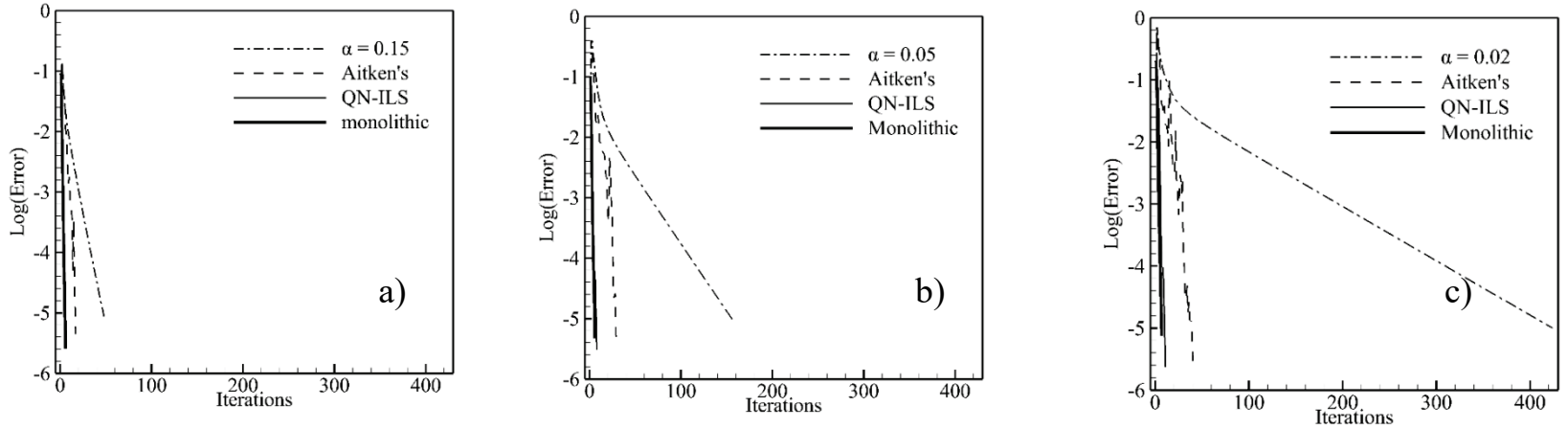

The history of convergence a) $\bar{\rho} = 10$, b) $\bar{\rho} = 1.2$, c) $\bar{\rho} = 0.5$

[3] S. Kang et al, 2012 , Investigation of fluid–structure interactions using a velocity-linked P2/P1 finite element method and the generalized- a method, International Journal for Numerical Methods in Engineering. vol. 90. pp:1539-1547.

Semi-monolithic method (version 3 FSI)

Performance of Semi-monolithic versus the full Monolithic method

A 2D flexible beam behind a cylinder

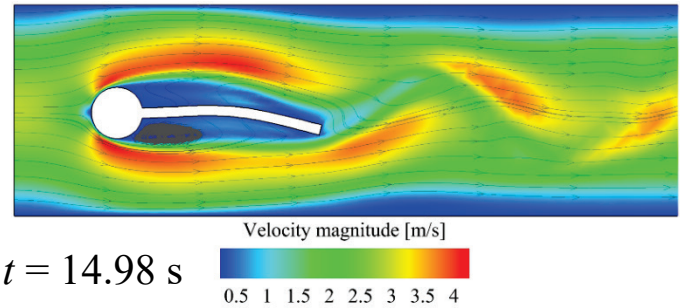

$t = 14.98$ s

CPU times (s) for one time-step (2D).

Case	Full monolithic	Semi-monolithic
$\bar{\rho} = 1$	1.32 **(4.23)**	0.312 **(1.0)**
$\bar{\rho} = 10$	1.179 **(4.17)**	0.283 **(1.0)**

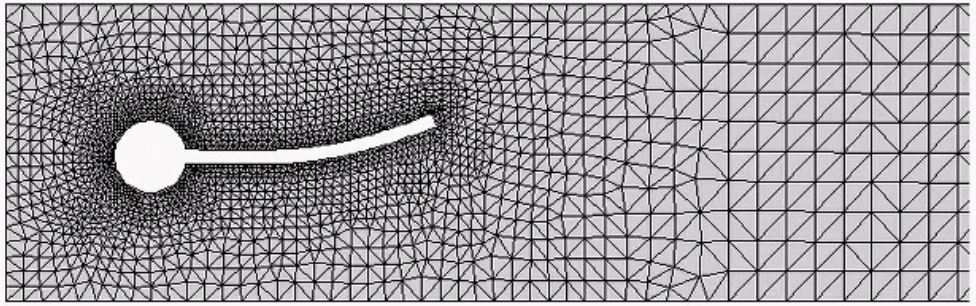

3D benchmark problem

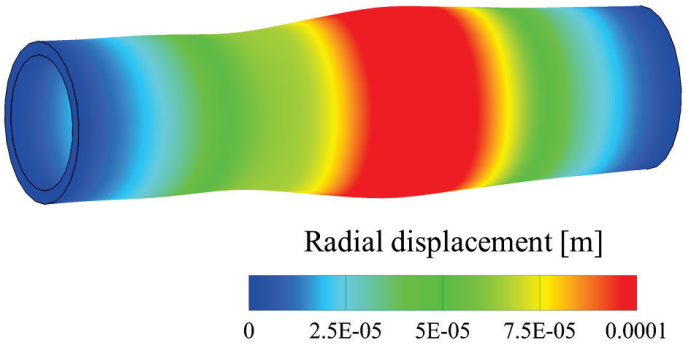

$t = 0.008$ s

CPU times (s) for one time-step (3D).

Case	Full monolithic	Semi-monolithic
$\bar{\rho} = 1$	159.68 **(2.82)**	56.58 **(1.0)**
$\bar{\rho} = 10$	151.58 **(2.84)**	53.31 **(1.0)**

Applications

- 1. FSI Simulation for Carotid Flow
- 2. FSI Simulation for Flow-Regulator
- 3. FSI Simulation for Artificial aortic valve

Blood flow interaction with a vessel in a carotid bifurcation of a rat

Elastic wall

Rigid wall

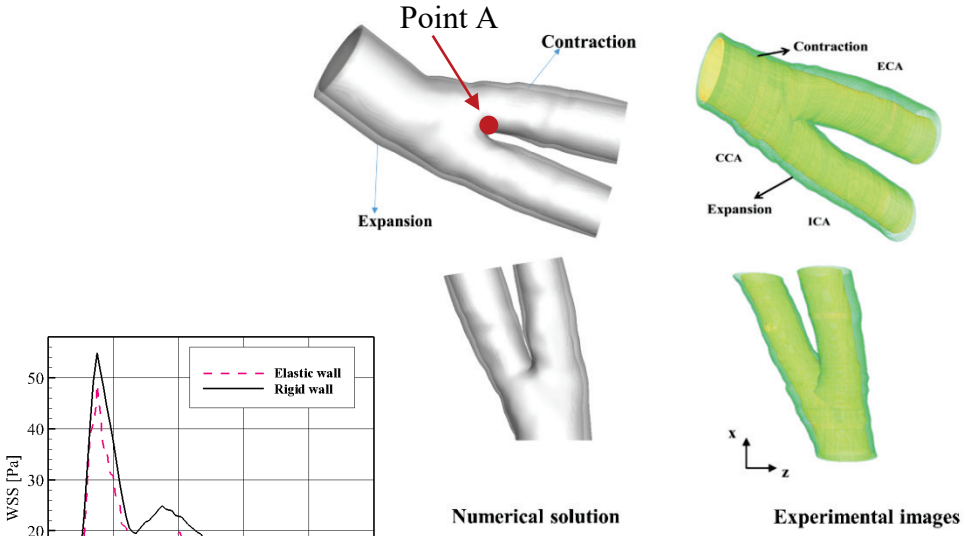

Comparison the vessel wall deformation obtained by numerical solution and the experimental data [17]

WSS of a point A at branch

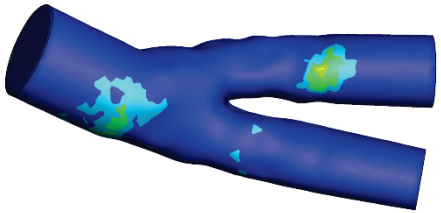

Oscillatory shear index

[17] Yeom et al. 3D reconstruction of a carotid bifurcation from 2D transversal ultrasound images, *Ultrasonics* 54.8 (2014): 2184-2192.

Blood flow interaction with a vessel in a carotid bifurcation of a rat

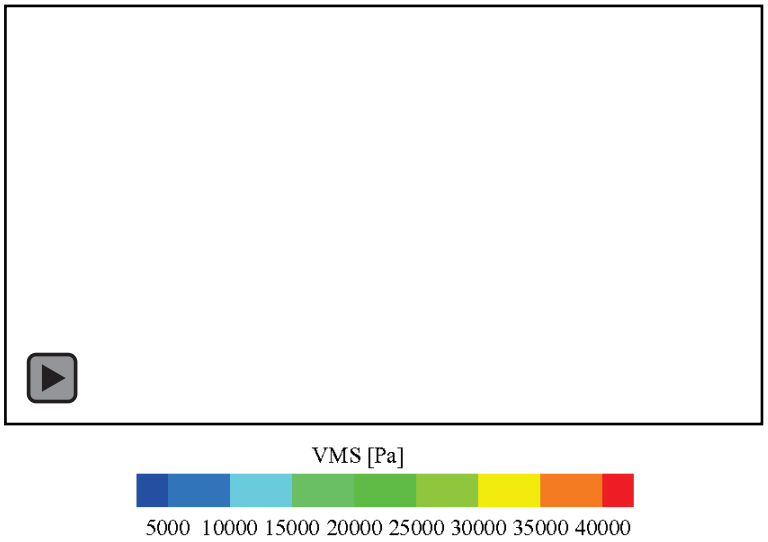

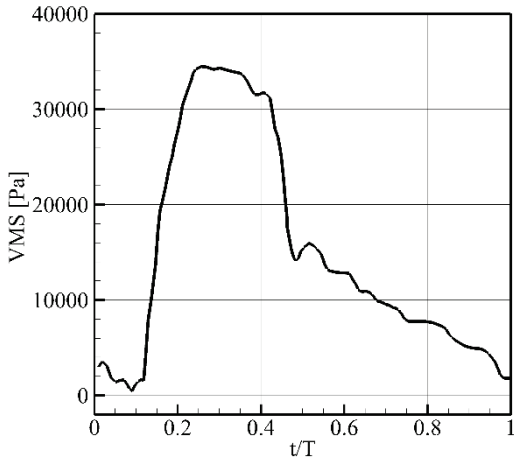

VMS of a point M at branch

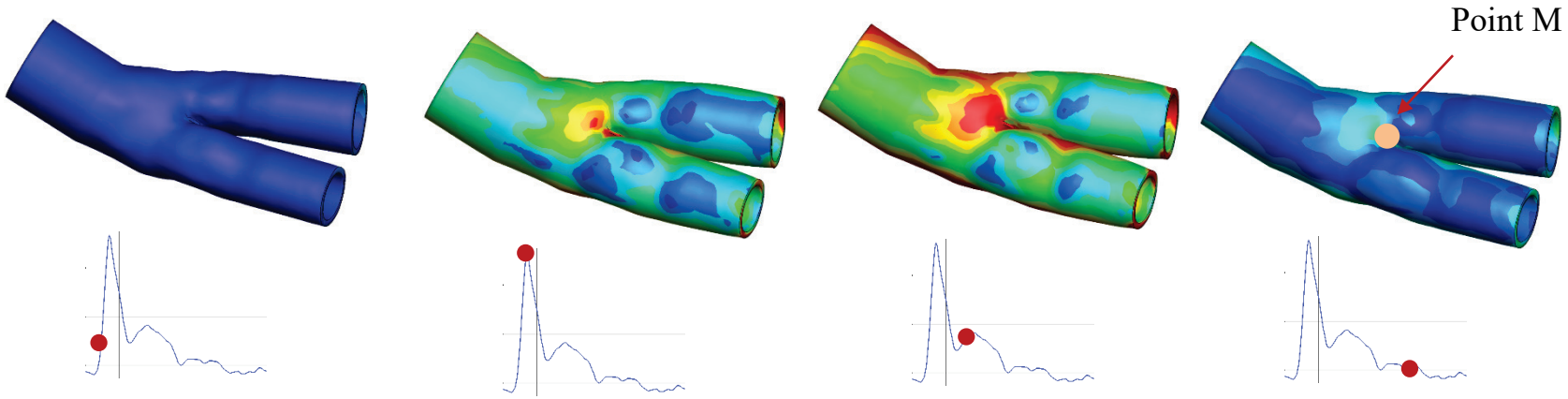

Simulation for Flow-Regulator

Schematics of Flow-Regulator

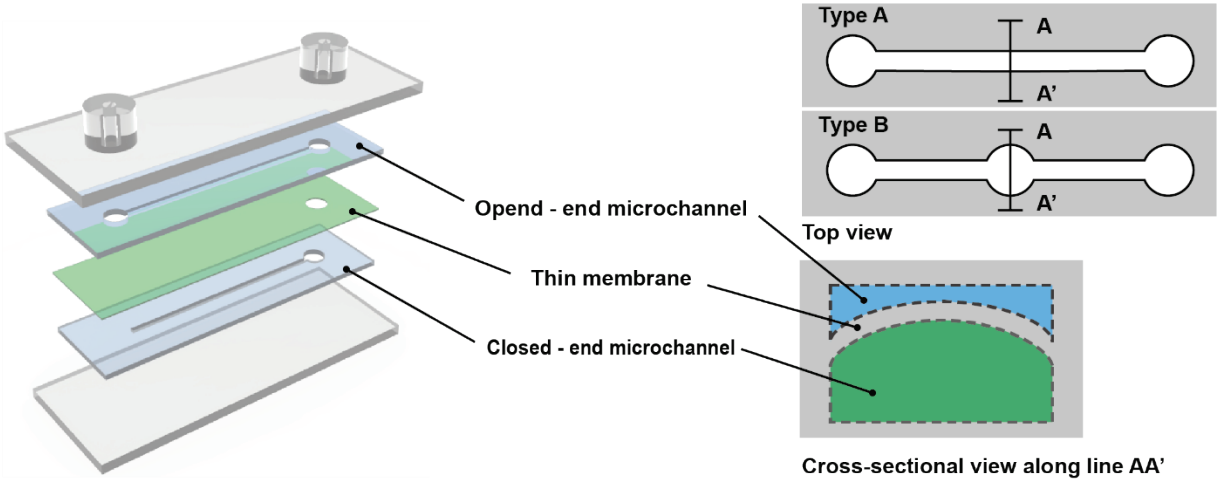

Geometry and mesh for simulation of Flow-Regulator

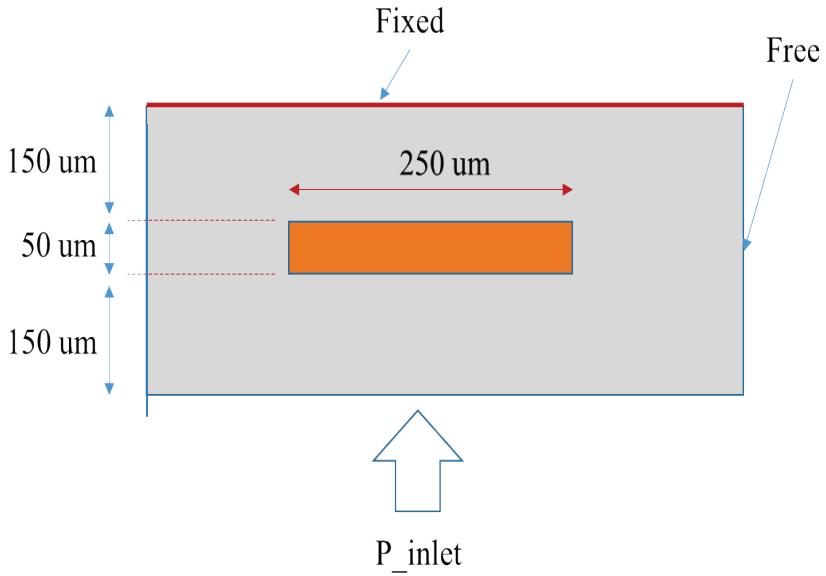

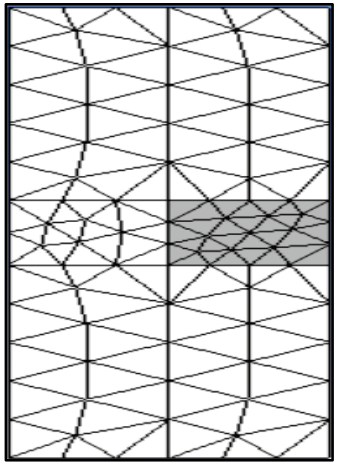

Unstructured mesh (half domain)

Simulation for Flow-Regulator

Comparison of numerical and the experimental result

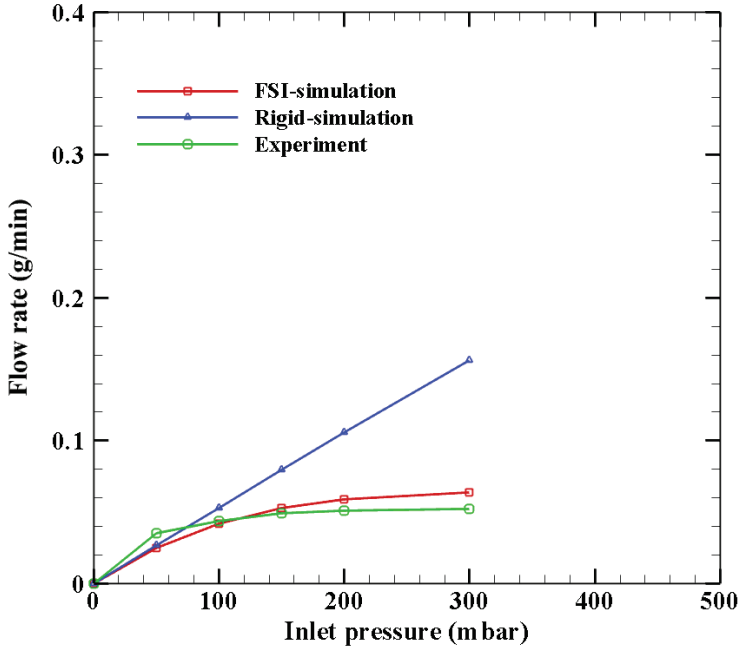

Cross sectional area at the symmetry plane of the channel for different inlet pressures (w = 250 μm, h = 50 μm)

(x* = X/100)

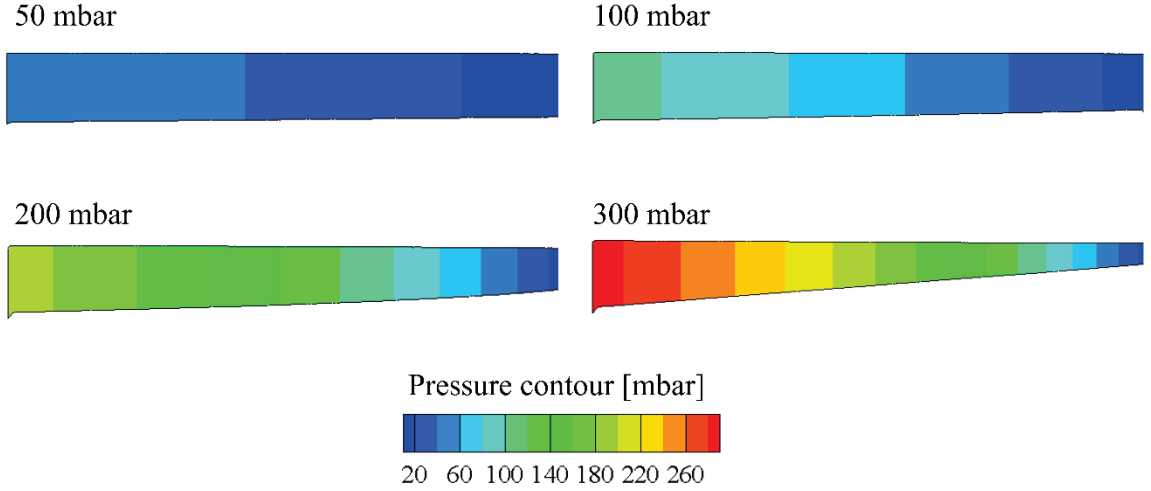

Simulation for Artificial aortic valve

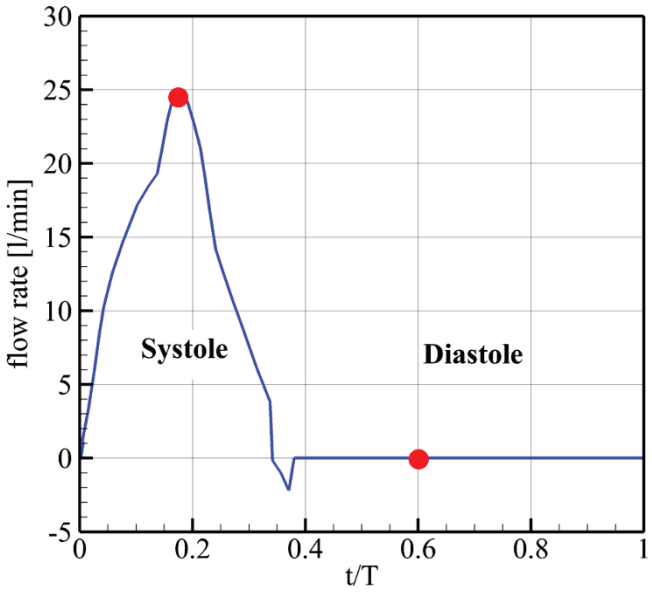

Flow rate at the inlet

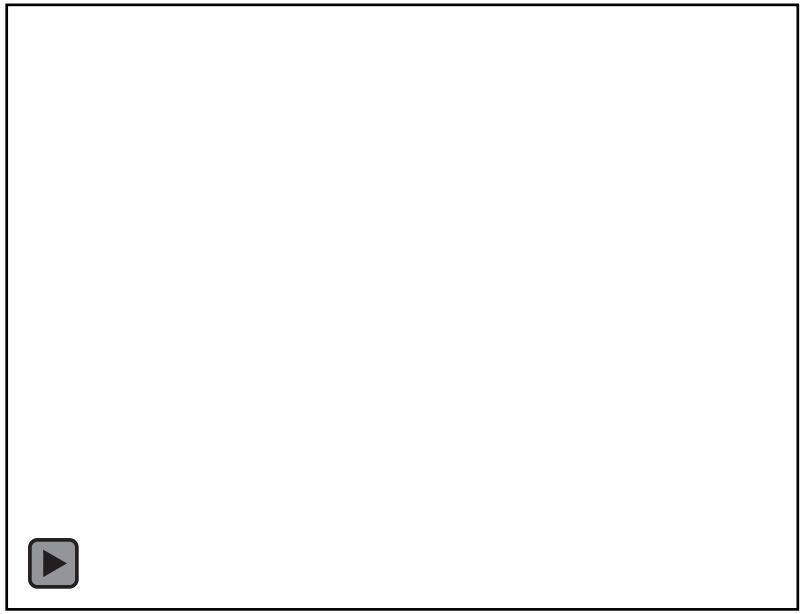

Unstructered grid

Interpolation for pressure (P1 element)

Interpolation for velocity (P2 element)

Area shape function

$N_a = S_a/S$

$N_b = S_b/S$

$N_c = S_c/S$

$S = S_a + S_b + S_c$

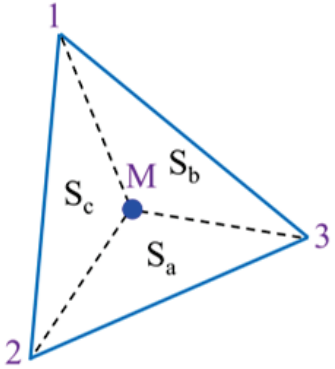

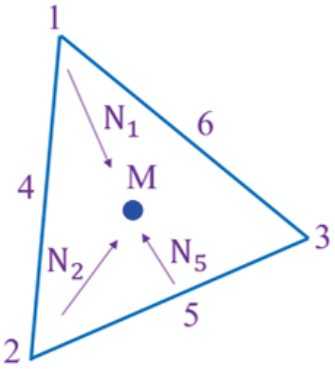

$$N_1 = N_a(2N_a - 1); \quad N_2 = N_b(2N_b - 1); \quad N_3 = N_c(2N_c - 1);$$

$$N_4 = 4N_aN_b; \quad N_5 = 4N_bN_c; \quad N_6 = 4N_cN_a;$$

Simulation for Artificial aortic valve

Animation of WSS

Animation of VMS

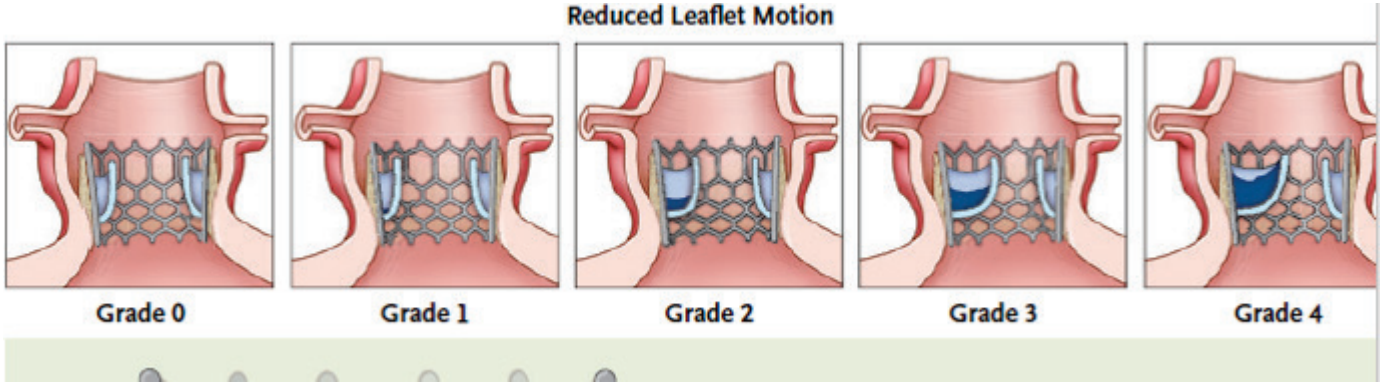

Recently development of FIV for nuclear reactor [1,2]

Numerical methods

- Nek5000 code based on spectral element method (using LES model of fluid flow in a Helical Steam Generators (SG))
  - Mesh: 407,364 hexahedral elements, ~137 million DOFs (7'th-order polynomial order). Re~ 8000.
  - AMG method is used to precondition the pressure step solver.

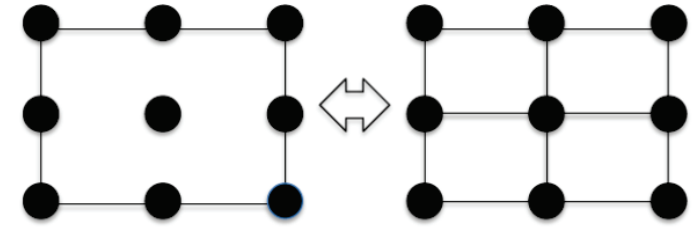

Nek5000 quad-9 surface representation (equivalent to a polynomial order equal to 2)

Diablo quad-8 surface representation

Schematic representation of the exchange of information on the two codes

- Diablo code is used for structural model.
  - The tubes are modeled by using four-node quadrilateral elements of two-dimensional shell. Support structures are modeled by using eight-node hexahedral elements (3,691,464 nodes and 3,595,200 elements).
  - Matric is ill condition -> Direct solver is employed.
  - Linear material for structure model (E =203 Gpa, ν=0.275, ρ=8060 kg/m^3), $\Delta t = 5\text{x}10^{-5}$ ($T_c \sim 2\text{x}10^{-4}$)

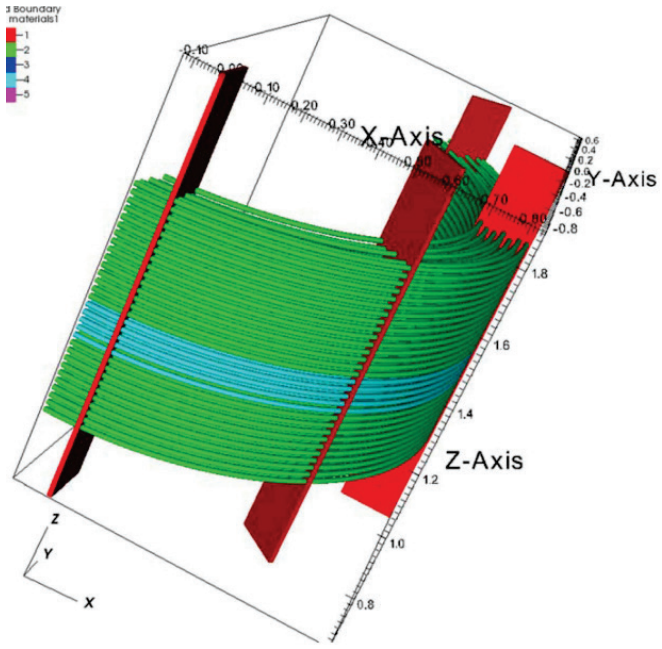

Computational model of the helical SG

- One-way coupled method is used for SG problem: (Nek5000 code -> Fluid load -> Diablo codes).
- Two-way coupled method for a high velocity problem:

$$\mathbf{u}_{\mathrm{FSI}}^{new} = \alpha \mathbf{u}_{\mathrm{FSI}}^{actual} + (1-\alpha)\mathbf{u}_{\mathrm{FSI}}^{old}$$

Fictitious mass and damping [2] are employed to improve the performance of the fixed under-relaxation scheme.

[1] Merzari et al., High-Fidelity Simulation of Flow-Induced Vibrations in Helical Steam Generators for Small Modular Reactors, nuclear technology, 2019.
[2] Merzari et al., A high-fidelity approach for the simulation of flow-induced vibration , Proceedings of the ASME 2016 Fluids Engineering meeting, USA.

Limitations of the method

❖ **One-way coupling**:

"At high flow condition, when deformations become significant, the one-way coupled approach is no longer adequate, and tight coupling is required".

❖ **Two-way coupling method:**

- Using the fixed under-relaxation scheme. The convergence is improved by employing the fictitious mass and damping technique. However, it is sill slow compared to the Newton based of strong-coupling method or a semi-implicit scheme.
- Using fictitious mass and damping -> two parameters tuning.

❖ ***One of the biggest limitations of Nek5000*** *is that it can use only hexahedral meshes. Generating full hexahedral meshes for a grid spacer geometry can be extremely challenging and time consuming since each block typically needs to be laid out manually*

In case of unstructured mesh**, tet-to-hex conversion** is necessary. A tetrahedral mesh was created first to describe the geometry, and then this mesh was converted to a hexahedral mesh. In this way, one tetrahedral element is divided into four hexahedral elements.

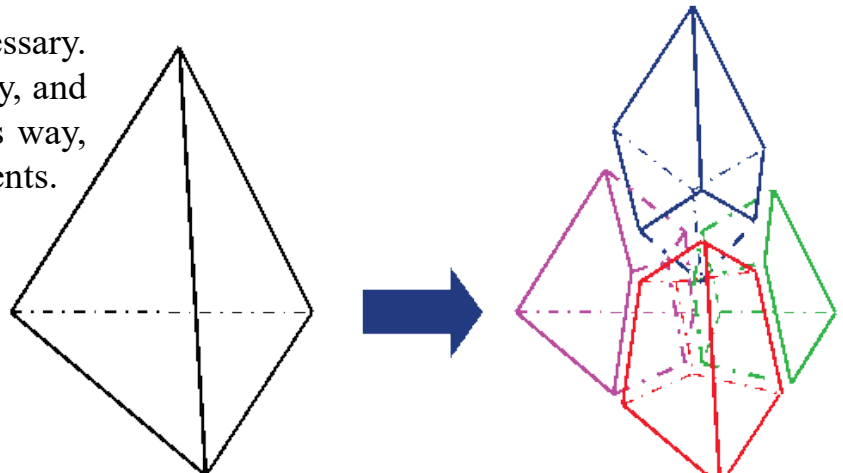

❖ **Diablo** code: solid simulation is based on (small deform) linear-elastic.

A new FIV code for nuclear reactor

- Improvement of FSI coupling by employing a **new semi-implicit scheme**. The simulation cost will be much cheaper.

- A new **Geometric multi-grid method** is used to solve the pressure equation. We have been developed a MG method for elliptic equations with a nearly optimal convergence. With 7 levels of MG, we can efficiently solve a problem of 100 million nodes (~ 50 nodes on the coarsest level)
- In case of ~100 million DOFs, -> MG is more than 50 times faster than CG -> **Must use MG.**

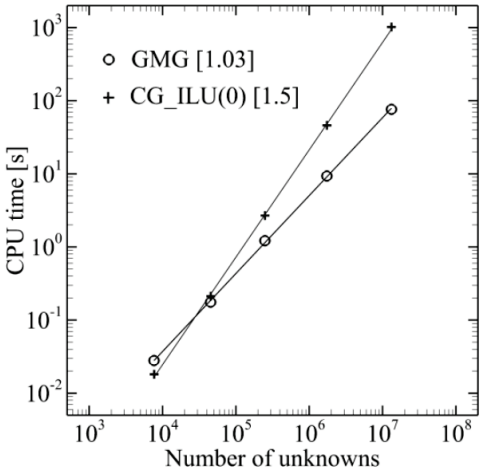

Results for 3D elliptic equation [4]

- **A Discontinuous Galerkin (DG) method** is developed for high-order computation with tetra element for unstructured grid to avoid the limitation of the Nek5000 code.

-**HDG is a highly scalable method**(Fully explicit scheme for momentum Eq.)

[4] S.T. Ha, H.G. Choi, A meshless geometric multigrid method based on a node-coarsening algorithm for the linear finite element discretization, Computers & Mathematics with Applications, 2021

Conclusions

- 밀도비(고체밀도/유체 밀도)가 크지 않은 경우에는 부가질량의 영향이 크므로, 분리기법(Partitioned method)의 사용할 때는 효과적인 알고리즘을 선택해야 함.

- 반일체(semi-monolithic)공식화는 분리기법(partitioned method)과 일체화(monolithic) 기법의 특성을 혼용한 방법으로, 제안된 기법들 중에서 안정성과 속도면(mono의 3~4배)에서 최고의 성능을 보여줌.

- 다만, 반일체(semi-monolithic)공식화는유체의 압력과 고체변수들이 연성된 식을 풀어야 하므로, scalable한 병렬화 기법의 구현에 복잡성이 존재하므로, 이에 대한 후속연구가 요구됨.

Extra slides

Hybridized Discontinuous Galerkin Method

The incompressible Navier-Stokes equations:

By introducing gradient tensor: $\mathbf{L} = \nabla \mathbf{u}$

$$\begin{cases} \mathbf{L} = \nabla \mathbf{u}, \text{in } \Omega \\ \dfrac{\partial \mathbf{u}}{\partial t} + \nabla \cdot (\mathbf{u} \otimes \mathbf{u}) - \nu \nabla \cdot \mathbf{L} + \nabla p = \mathbf{f}, \text{in } \Omega \\ \nabla \cdot \mathbf{u} = 0, \text{in } \Omega \\ \mathbf{u} = \mathbf{g}, \text{on } \partial\Omega \end{cases}$$

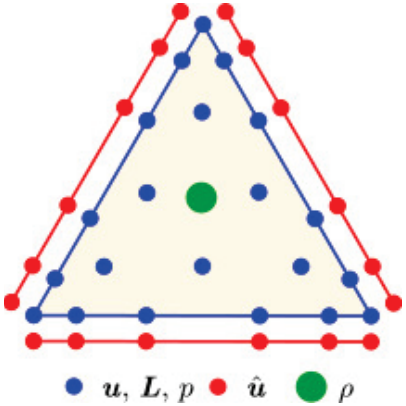

Local unknowns

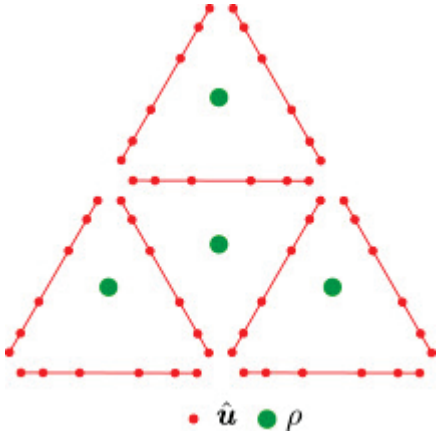

Global unknowns

We seek an approximation $(\mathbf{L}_h^n, \mathbf{u}_h^n, p_h^n, \hat{\mathbf{u}}_h^n) \in \mathbf{G}_h \times \mathbf{V}_h \times \mathbf{P}_h \times \mathbf{M}_h(\mathbf{g})$ such that

$$(\mathbf{L}_h^n, \mathbf{G})_{\Omega_h} + (\mathbf{u}_h^n, \mathbf{G})_{\Omega_h} - \langle \hat{\mathbf{u}}_h^n, \mathbf{G}\mathbf{n} \rangle_{\partial\Omega_h} = 0$$

$$\left(\frac{\partial \mathbf{u}_h^n}{\partial t}, \mathbf{v}\right)_{\Omega_h} + (\nu \mathbf{L}_h^n - p_h^n \mathbf{I} - \mathbf{u}_h^n \otimes \mathbf{u}_h^n, \nabla \mathbf{v})_{\Omega_h} + \left\langle \left(-\nu \hat{\mathbf{L}}_h^n + \hat{p}_h^n \mathbf{I} + \hat{\mathbf{u}}_h^n \otimes \hat{\mathbf{u}}_h^n\right)\mathbf{n}, \mathbf{v} \right\rangle_{\partial\Omega_h} = (\mathbf{f}, \mathbf{v})_{\Omega_h}$$

$$-(\mathbf{u}_h^n, \nabla q)_{\Omega_h} + \langle \hat{\mathbf{u}}_h^n \cdot \mathbf{n}, q \rangle_{\partial\Omega_h} = 0$$

$$\left\langle \left(-\nu \hat{\mathbf{L}}_h^n + \hat{p}_h^n \mathbf{I} + \hat{\mathbf{u}}_h^n \otimes \hat{\mathbf{u}}_h^n\right)\mathbf{n}, \boldsymbol{\mu} \right\rangle_{\partial\Omega_h} = 0$$

$$(p_h^n, \mathbf{1})_{\Omega_h} = 0$$

for all $(\mathbf{G}, \mathbf{v}, q, \boldsymbol{\mu}) \in \mathbf{G}_h \times \mathbf{V}_h \times \mathbf{P}_h \times \mathbf{M}_h(\mathbf{0})$ where the numerical trace is defined as

$$-\nu \hat{\mathbf{L}}_h^n + \hat{p}_h^n \mathbf{I} + \hat{\mathbf{u}}_h^n \otimes \hat{\mathbf{u}}_h^n = -\nu \mathbf{L}_h^n + p_h^n \mathbf{I} + \hat{\mathbf{u}}_h^n \otimes \hat{\mathbf{u}}_h^n + \mathbf{s}_h(\mathbf{u}_h^n, \hat{\mathbf{u}}_h^n)$$

Hybridized Discontinuous Galerkin Method

Local solver

$$\begin{bmatrix} \mathbf{A}_{uu} & \mathbf{A}_{uL} & \mathbf{A}_{up} & 0 & \mathbf{A}_{u\hat{u}} & \mathbf{A}_{u\rho} \\ \mathbf{A}_{Lu} & \mathbf{A}_{LL} & 0 & 0 & \mathbf{A}_{L\hat{u}} & \mathbf{A}_{L\rho} \\ \mathbf{A}_{pu} & 0 & 0 & \mathbf{A}_{\rho p}^{\mathrm{T}} & \mathbf{A}_{p\hat{u}} & 0 \\ 0 & 0 & \mathbf{A}_{\rho p} & 0 & 0 & -\mathbf{1} \\ \mathbf{A}_{\hat{u}u} & \mathbf{A}_{\hat{u}L} & \mathbf{A}_{\hat{u}p} & 0 & \mathbf{A}_{\hat{u}\hat{u}} & 0 \\ 0 & 0 & 0 & 0 & \mathbf{A}_{\rho\hat{u}} & 0 \end{bmatrix} \begin{Bmatrix} \mathbf{u} \\ \mathbf{L} \\ p \\ \lambda \\ \hat{\mathbf{u}} \\ \rho \end{Bmatrix} = \begin{bmatrix} \mathbf{f} \\ 0 \\ 0 \\ 0 \\ \mathbf{t} \\ 0 \end{bmatrix}$$

Global solver involves only:

+) $\hat{\mathbf{u}}$: velocity trace (defined on face of element)

+) ρ : mean of the pressure in each element

Local solver: element solution

+) computed in element-by-element fashion

Saddle-point system $\mathbf{G}\mathbf{E}^{-1}\mathbf{H}\boldsymbol{\rho} = \mathbf{E}^{-1}\mathbf{r}$

Solve Global system for: $\hat{\mathbf{u}}$, ρ

Static condensation

$$\begin{bmatrix} \mathbf{A} & \mathbf{B} \\ \mathbf{C} & \mathbf{D} \end{bmatrix} \begin{Bmatrix} \mathbf{z}_1 \\ \mathbf{z}_2 \end{Bmatrix} = \begin{bmatrix} \mathbf{r}_1 \\ \mathbf{r}_2 \end{bmatrix} \Rightarrow \begin{array}{l} \mathbf{z}_1 = -\mathbf{A}^{-1}\mathbf{B}\mathbf{z}_2 + \mathbf{A}^{-1}\mathbf{r}_1 \\ (-\mathbf{C}\mathbf{A}^{-1}\mathbf{B} + \mathbf{D})\mathbf{z}_2 = \mathbf{r}_2 - \mathbf{C}\mathbf{A}^{-1}\mathbf{r}_1 \end{array} \Leftrightarrow \underbrace{\begin{bmatrix} \mathbf{A} & \mathbf{B}^{\mathrm{T}} \\ \mathbf{B} & 0 \end{bmatrix} \begin{Bmatrix} \hat{u} \\ \rho \end{Bmatrix} = \begin{bmatrix} \mathbf{r}_e \\ 0 \end{bmatrix}}_{\text{Elemental system}}$$

Assembly $\Rightarrow$ $\underbrace{\begin{bmatrix} \mathbf{E} & \mathbf{H} \\ \mathbf{G} & 0 \end{bmatrix} \begin{Bmatrix} \hat{u} \\ \rho \end{Bmatrix} = \begin{bmatrix} \mathbf{r} \\ 0 \end{bmatrix}}_{\text{Global system}}$

Example: Kovasznay flow

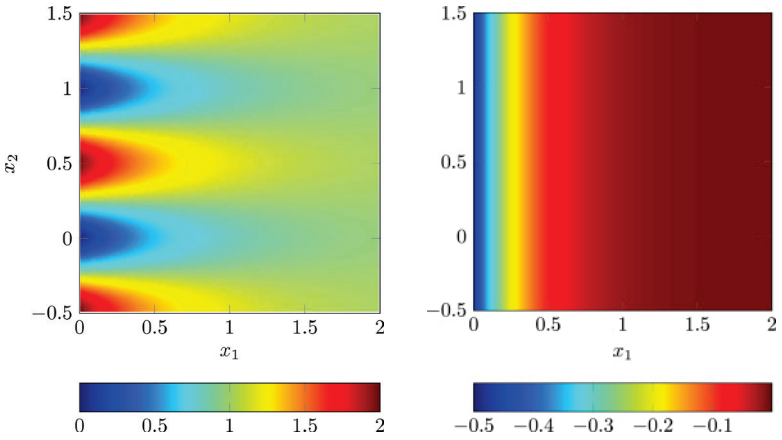

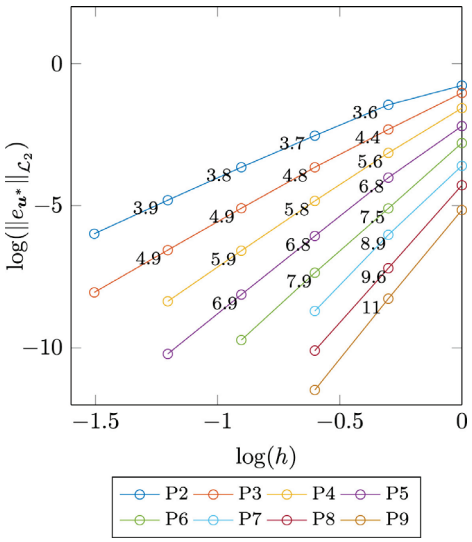

Convergence of velocity O(p+2)

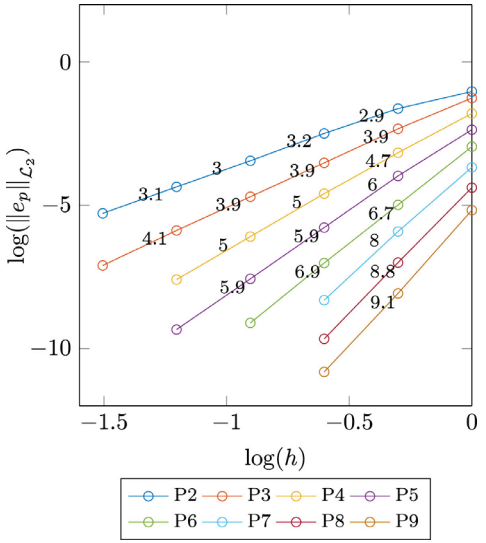

Convergence of pressure O(p+1)

High-order DG method for turbulent flows

Discontinuous Galerkin method for incompressible turbulent flows

References	Model
N. Fehn et al., [1], C. C. de Wiart et al., [2]	LES
G. Noventa et al., [3], A. Crivellini et al. [4]	RANS
B. Krank et al., [5], F. Bassi et al., [6]	DNS and LES
F. Bassi et al. [7], B. Landmann et al. [8]	RANS and k-ω

Hybridized Discontinuous Galerkin method for compressible turbulent flows

References	Model
P. Fernandez et al. [9]	LES

Example: Turbulent channel flows with DG method [5]

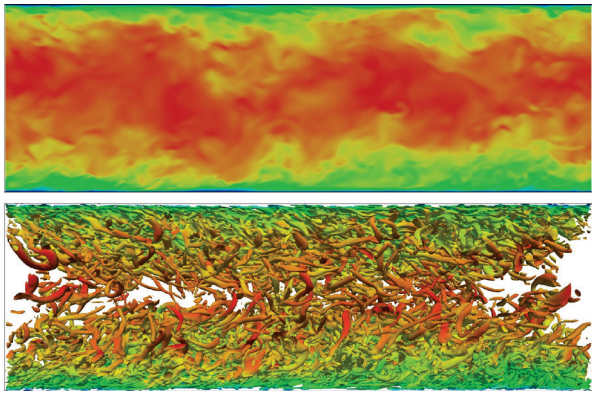

Velocity magnitude and eddies for $Re_\tau = 590$

Case	$N_{e,1} \times N_{e,2} \times N_{e,3}$	k	$nDoFs$
$ch180\_N32^3\_k5\_V3c\_dns$	$32 \times 32 \times 32$	5	28e6
$ch590\_N64^3\_k4\_V3c\_dns$	$64 \times 64 \times 64$	4	131e6
$ch180\_N8^3\_k3\_V3c\_les$	$8 \times 8 \times 8$	3	0.13e6
$ch180\_N16^3\_k3\_V\{3c,4\}\_les$	$16 \times 16 \times 16$	3	1.0e6
$ch180\_N32^3\_k3\_V3c\_les$	$32 \times 32 \times 32$	3	8.4e6
$ch590\_N16^3\_k4\_V\{3c,4\}\_les$	$16 \times 16 \times 16$	4	2.0e6
$ch590\_N32^3\_k4\_V3c\_les$	$32 \times 32 \times 32$	4	16e6

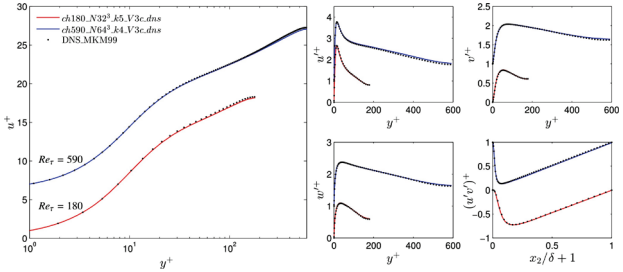

DNS with DG method

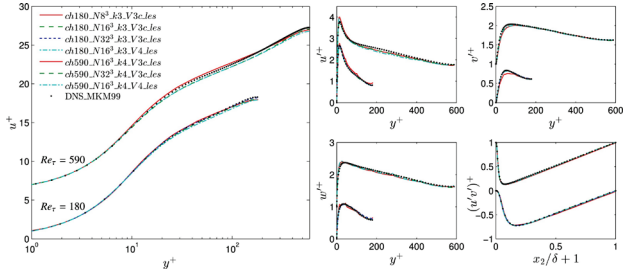

LES with DG method

[1] N. Fehn et al., JCP 372 (2018) 667-693; [2] C. C. de Wiart et al., IJNMF 78 (2015) 335-354; [3]G. Noventa et al., C&F139 (2016) 248-260; [4] A. Crivellini, C&F 81 (2013) 122-133; [5] B. Krank et al., JCP 348 (2017) 634-659; [6] F. Bassi et al., European J. of Mechanics B/Fluids 55 (2016) 367-379; [7] F. Bassi et al., Computers and Fluids 98 (2014) 54-68; [8] B. Landmann et al., C&F 37 (2008) 427-438; [9] P. Fernandez et al., JCP 336 (2017) 308-329.

Fictitious mass and damping [2]

"When added-mass effects are prominent, under-relaxations schemes such as that used here may require small values of ω and large number of iterations to converge. In order to improve the convergence behavior, fictitious mass and damping are employed as in. Additional traction terms are added to the solid solver, based on a fictitious surface mass density $\boldsymbol{f_m}$ and fictitious surface damping density $\boldsymbol{f_d}$, such that the total surface traction is evaluated by using the surface accelerations and velocities evaluated between consecutive iterations $\mathbf{u}_i^{n+1}$, $\mathbf{u}_{i-1}^{n+1}$"

$$\mathbf{t}^{n+1} = \mathbf{t}_{FSI}^{n+1} - \mathbf{n}f_m\left[\left(\mathbf{u}_i^{n+1} - \mathbf{u}_{i-1}^{n+1}\right)\bullet\mathbf{n}\right] - \mathbf{n}f_d\left[\left(\mathbf{u}_i^{n+1} - \mathbf{u}_{i-1}^{n+1}\right)\bullet\mathbf{n}\right]$$

$$\mathbf{t}_{FSI}^{n+1} = -p^{n+1}\mathbf{n} + \upsilon\left(\nabla^S\mathbf{v}^{n+1}\right)\bullet\mathbf{n}$$

*"The added mass terms **affect only the convergence of the iterative scheme**, at convergence they evaluate to zero. The fictitious terms f_m and f_d are tuning parameters"*

Total Lagrangian and Updated Lagrangian formulations

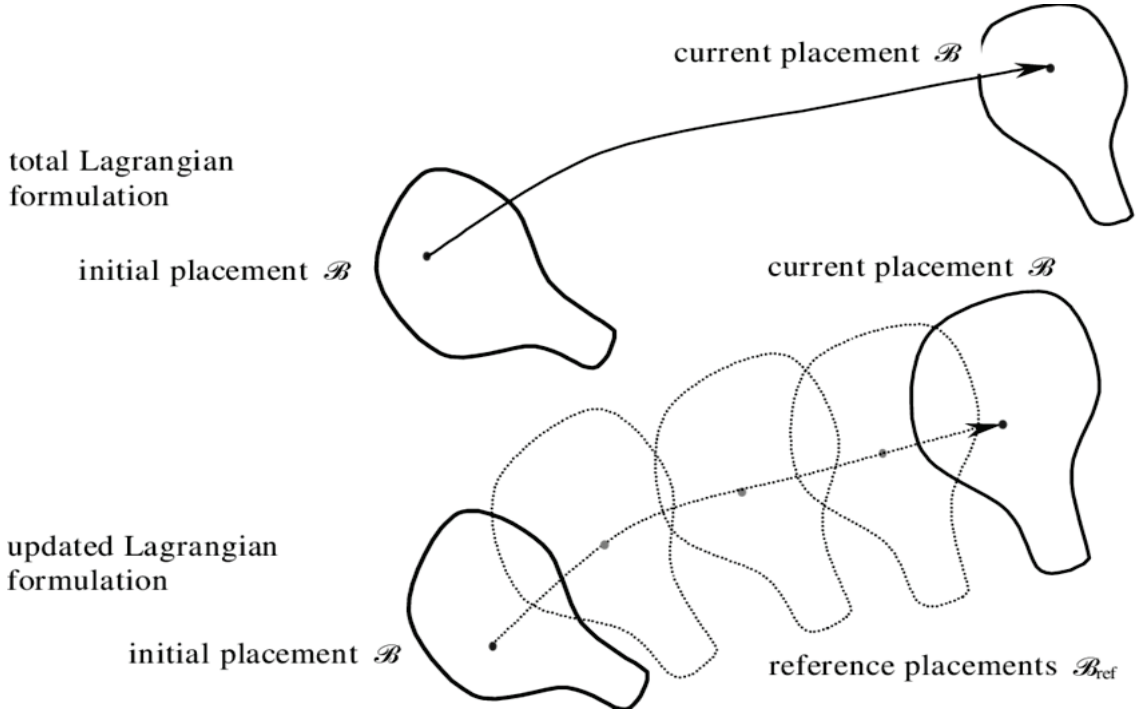

Total Lagrangian ->

$$\int_{{}^0V} {}^{t+\Delta t}_{0}S_{ij}\ \delta\, {}^{t+\Delta t}_{0}\epsilon_{ij}\ d{}^{0}V = {}^{t+\Delta t}\mathcal{R}$$

all variables being referred corresponding to the initial configuration at time t=0

Updated Lagrangian->

$$\int_{{}^tV} {}^{t+\Delta t}_{t}S_{ij}\ \delta\, {}^{t+\Delta t}_{t}\epsilon_{ij}\ d{}^{t}V = {}^{t+\Delta t}\mathcal{R}$$

all variables being referred corresponding to the last calculated configuration.